

# Development of an *In Vitro* Method for Modeling Drug Release and Subsequent Tissue Drug Uptake and Deposition in a Pulsatile Flow Network

Caroline C. O'Brien, Charles H. Finch, Penny Martens, Tracie J. Barber and Anne Simmons

**Abstract**—A novel benchtop model of drug elution and arterial drug deposition following stent implantation has been developed. The model contains a single drug loaded strut and a compartment simulating the vessel wall, housed in a flow chamber under a pulsatile flow regime. Each component has programmable transport properties that can be implemented into a computational model of drug elution. An initial experiment determining the effects of luminal flow on drug deposition patterns was performed. The results show that spatial distribution of drug correlates with areas of low and recirculating flow surrounding the strut. This spatial distribution of drug was shown to be dependent on both transient release behavior and the local flow field surrounding the strut. Furthermore, these results showed that the novel method could be used to study the effects of luminal flow in the presence of single or multiple struts. The method could also be used to explore more complex drug release strategies.

## I. INTRODUCTION

THE drug eluting stent (DES) provides a platform for the delivery of anti-proliferative drugs. The biologic effect and therefore the success of this form of drug therapy lies in its ability to deliver therapeutically effective levels of drug to the site of the vessel where restenosis occurs. Biologic outcome is determined by a series of mechanisms following implantation. Firstly, kinetics of the drug in the polymer drug carrier will determine the amount of drug released from the strut coating [1]. From here, drug will be delivered directly to the vessel wall or to the blood stream where convective and diffusive forces will carry it to the mural interface for a secondary source of drug uptake [2]. The spatial drug distribution is governed primarily by the tissue's own transport forces, however these will be modulated by other secondary factors such as tissue and drug physicochemical properties. For example, protein transport will facilitate diffusion circumferentially [3] while hydrophobic interactions can lead to significantly large spatial variation in concentration [4, 5]. The amount of drug retained, and therefore the biologic outcome, is a function of this transient drug distribution and the type and number of binding sites.

A novel benchtop experiment has been constructed to

determine the spatial drug distribution in the fluid and tissue as a result of this primary mechanism of transport. The aim is therefore to characterize the drug release behavior from the stent coating and the corresponding luminal and tissue drug uptake and distribution as a result of convective and diffusive mass transport. From this experiment real-time images of transient release phenomena in a dynamic flow field and resulting spatial tissue drug distribution are able to be acquired. A 2D reconstruction of a stent strut placed on a model vascular bed was created using a drug-loaded elastomer as a model of a drug-coated wire, a hydrogel to replicate a vessel wall and pulsatile flow of a blood mimicking fluid.

This *in vitro* design will eventually be used to validate a computational method which requires transport properties of the *in vitro* system to be determined. These properties include diffusion coefficients of the marker drug through the working fluid and hydrogel, permeability and mesh size of the hydrogel and drug release behavior of the drug loaded elastomer. It follows earlier computational analyses, validated *in vivo*, that use continuum analysis to simulate this system of drug delivery [2]. Taken together, this computational and *in vitro* model will present a unique method for which to analyze transient behavior of local drug delivery and therefore aid in the development of more efficient and safe DES design, manufacture and clinical protocol.

## II. EXPERIMENTAL METHODS

### A. Flow Chamber and Apparatus

As shown in Fig. 1, the acrylic flow channel has a 2D configuration of strut and porous tissue positioned so as to isolate the effects of flow parameters on the flow recirculation areas upstream and downstream of the model stent strut. Channel dimensions were chosen to guarantee developed flow for all future experimental Reynolds and Womersley number variations [6].

The tissue was modeled as a permeable membrane, using a poly (vinyl alcohol) (PVA) hydrogel housed in a recess midway along the channel. A strut loaded with fluorescently labeled drug was then placed over the hydrogel and a pulsatile flow was allowed to enter the channel. Both the acrylic channel and hydrogel are optically clear so resolution of fluorescence intensities is maximized. The properties of

C. C. O'Brien, C.H. Finch, P. Martens, T. J. Barber and A. Simmons are with the Graduate School of Biomedical Engineering, The University of New South Wales, Sydney, UNSW Australia 2052 (e-mail: caroline.obrien@student.unsw.edu.au).

all materials used were similar to physiological parameters, while also ensuring transient visualization and analysis were possible.

Flow was generated with a piston pump (CompuFlow 1000 MR, Shelley Medical Imaging Technologies, London, ON, CA) outputting a physiologically realistic flow waveform, taken from Moore Jr. et al. [7], and scaled to provide a Reynolds number of  $Re_0 = 427$ .

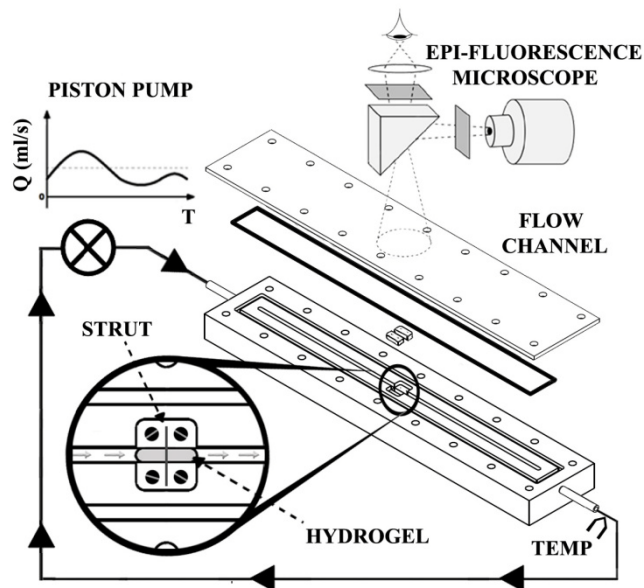


Fig. 1. Schematic of 2D strut showing placement of drug-loaded strut placed on a bed of hydrogel and secured in place by two plates, flush with each side of the flow channel of diameter  $D = 3$  mm. Flow is generated from a pulsatile flow pump, and visualization of drug contours is through an epi-fluorescence microscope.

### B. Working Fluid

The working fluid was glycerin/water 40/60 wt% mixture and 0.02% surfactant, sufficient for pump lubrication as well as providing properties consistent with blood. Density of this mixture was calculated as  $\rho = 1100$  kg/m<sup>3</sup> with a dynamic viscosity  $\mu = 4.394$  mPa.s [8], calculated for a temperature of 23°C. A thermocouple was located downstream to monitor temperature, and confirmed only small fluctuations ( $\pm 0.30^\circ\text{C}$ ) and therefore a relatively constant dynamic viscosity over the course of the experiment.

### C. Hydrogel Preparation

Hydrogels were fabricated from poly (vinyl alcohol) (PVA) (16kDa, 98% hydrolyzed) functionalized with 7 methacrylate crosslinkers (PVA-MA) using the method by Bryant et al. [9]. Macromer solution was prepared by dissolving 20 wt% PVA-MA in deionized water, with 0.05 wt% of the photoinitiator Irgacure 2959 (CIBA). The solution was then photopolymerised for 3 minutes ( $30$  mW/cm<sup>2</sup>,  $\lambda = 365$  nm) in a mould creating a membrane able to fit into the recess in the flow chamber. Once prepared, the hydrogels were swollen in a solution of working fluid for 48 hours to ensure removal of sol fraction.

### D. Marker Drug and Transport Properties

Fluorescein-Sodium (FS) (333 Da,  $\lambda_{\text{ex}} = 490$  nm /  $\lambda_{\text{em}} = 512$  nm), was chosen as the model drug in the system. Its hydrophilic properties and low molecular weight make it an excellent candidate for transport through PVA hydrogels and the chosen working fluid.

The diffusion coefficient of the marker drug FS in the free solution and the hydrogel was calculated using a “Side-Bi-Side” diffusion cells (PermeGear). In calculating the free solution diffusivity a hydrophilic filter (0.22  $\mu\text{m}$  pore diameter, 70% porosity, 125  $\mu\text{m}$  thickness, Millipore) was placed between the diffusion chambers. The pore size was at least two orders of magnitude larger than FS molecular radius and therefore allows free diffusion of FS in the glycerol water solution [10].

For the diffusivity of FS through the hydrogel, a PVA hydrogel membrane (15 mm dia, 1 mm thick) was used in the place of the filter paper.

The solute permeability coefficient,  $P$ , was calculated from the equation [11]:

$$\ln\left(1 - \frac{2c_t}{c_0}\right) = -\frac{2A}{V}Pt \quad (1)$$

where  $c_0$  is the initial solute concentration of the donor chamber and  $c_t$  is the solute concentration in the receptor chamber at time  $t$ .  $V$  is the chamber volume and the effective area for permeation  $A$  is equal to the porosity multiplied by the orifice area. The coefficient of diffusion,  $D$ , through an unbounded pore space is equal to the permeability,  $P$ , multiplied by membrane thickness,  $\delta$  [11].

### E. Preparation of drug loaded strut and characterization of drug release

For 2D analysis, a polyurethane elastomer was chosen as the drug carrier because of its ease of manufacture and adequate rigidity to maintain shape under experimental flow conditions. Drug loaded films, replicating a strut were cast from a 1% wt/wt solution of FS dissolved into a Pellethane (PU) + dimethylacetamide (DMA-c) solution. These films were cut yielding an aspect ratio of 6 (W:H).

A release study was performed to measure diffusion characteristics of the drug loaded polymer of thickness  $L$ . Diffusion coefficient  $D$  was approximated by [12]:

$$\frac{M_t}{M_\infty} \approx 4\sqrt{\frac{Dt}{L^2\pi}} \quad (2)$$

The total amount of drug released,  $M_t$ , was measured at time points  $t$  and compared to initial concentration  $M_\infty$ . The experiment was repeated threefold.

### F. Analysis

The accumulation of fluorescently labeled drug and its deposition in the tissue below the strut was detected using an inverted epi-fluorescence microscope (Nikon Eclipse TE2000). A 4X magnification lens was chosen, with real-time images acquired digitally with a CCD camera and Spot software. Images were taken at different time points with an exposure time of 55 ms. The experimental run time was approximated to be 3 hours.

Finally the strut was removed, the surface of the hydrogel flushed with clean working fluid and the hydrogel cut through the center plane. A cross-sectional image of the mural footprint of drug in the hydrogel was then acquired. All images were analyzed with ImageJ software and finally fluorescence was converted to concentration ( $\mu\text{g/mL}$ ) using a standard dilution curve. Experiments were run in triplicate.

### III. RESULTS

The diffusion coefficients of the hydrogel and the free solution under experimental conditions were determined to be  $1.9 \pm 0.5 \times 10^{-7} \text{ cm}^2/\text{s}$  and  $2.1 \pm 0.2 \times 10^{-7} \text{ cm}^2/\text{s}$  respectively. While it was expected that the free diffusivity would be greater than diffusion through a hydrogel membrane, the large volume fraction of working fluid and large mesh size of the PVA matrix offered little impedance to the solute and therefore variation between the two values was found to be small.

Drug release experiments found diffusivity of drug from the polyurethane coating was calculated as  $2.9 \pm 0.6 \times 10^{-10} \text{ cm}^2/\text{s}$ .

Results from the *in vitro* model are shown in Fig. 2(b). Drug pooling in the fluid in the regions proximal and distal to the strut is seen. Larger deposition is seen in the near wall region where flow is lower than at the centerline ( $y = 0$ ).

As shown in Fig. 2(a), drug concentration in both proximal and distal regions in the flow (measured as the area weighted average) increases with time. In Fig. 2(c), resultant footprints in the hydrogel show the surface spatial distribution to be skewed towards the proximal region of the strut. Area weighted average concentration in the distal segment of Fig. 2(c) was found to be on average  $4.52 \pm 1.45 \mu\text{g/mL}$  larger than in the proximal. In other words average deposition or total uptake in the distal segment of the hydrogel is actually larger than in the proximal side.

### IV. DISCUSSION AND CONCLUSION

The distribution of anti-proliferative agents in the tissue following stent implantation is determined primarily by physiologic transport forces [5]. While local tissue architecture, in particular binding sites and hydrophobic and hydrophilic interactions, will contribute their own forces, these mechanisms will only be secondary and therefore will only act to modulate the primary distribution established from processes of convection and diffusion.

The present study is concerned with characterizing the primary drug distribution as a result of these convective and diffusive forces. The temporal window in which to characterize these features is limited by several experimental factors.

While the diffusivity of FS in PVA hydrogels was close to *in vivo* diffusion of paclitaxel in tissue [4], differing only by an order of magnitude, there were some fundamental differences. Both FS and the PVA hydrogel are hydrophilic while in reality hydrophobic drugs used in DES like paclitaxel and sirolimus will partition in the tissue. In

addition the hydrogel offers no binding sites like tissue does, in which case highly diffusible drugs like Fluorescein-sodium will rapidly diffuse through the medium, in which case there will be a limited timeframe in which to capture this primary distribution of drug in the hydrogel bed.

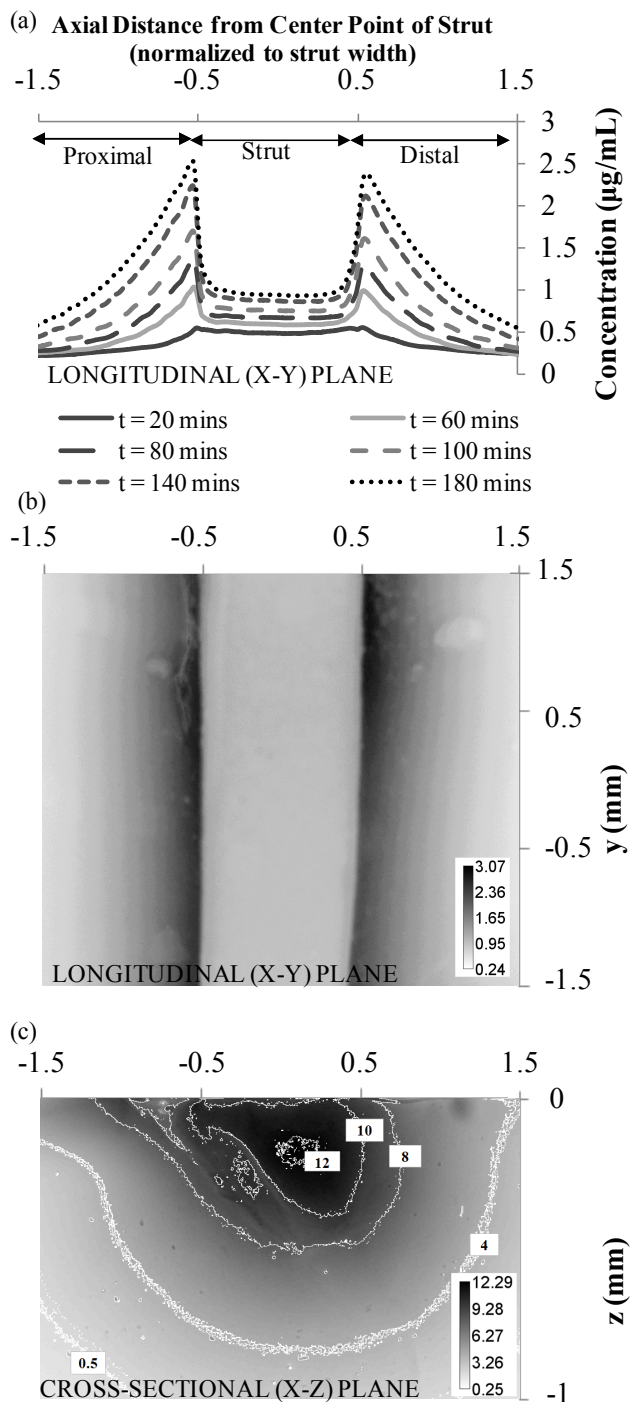


Fig. 2. Results from *in vitro* experiment. Each figure is shown against axial distance normalized to strut width, where  $x = 0$  denotes centre point of strut. (a) Transient drug concentration in the flow, measured over the axial distance and averaged over the height of channel; (b) Fluorescent image of drug accumulation in areas surrounding strut showing contours of drug concentration ( $\mu\text{g/mL}$ ); (c) Cross section of hydrogel following stent removal at 180 minutes showing contours of drug concentration ( $\mu\text{g/mL}$ ). Major contour levels are also marked.

Furthermore drug uptake into the flow and the hydrogel will vary with different release rates. For instance, a bolus release of drug will be cleared away almost immediately by the flow before it can be absorbed by the tissue, while a slow release will result in a limited amount of drug accumulating in the lumen. The choice of a polyurethane as a carrier for the model drug resulted in a fast but sustained release of drug over a 3 hour interval. Local stent based drug delivery is of the order of days, a time of which is unrealistic and, indeed, unnecessary for an efficient *in vitro* experiment. The temporal window of 3 hours for this experimental setup was found to be sufficient for accurate resolution of transient drug transport from the strut, in the fluid and in the hydrogel.

This study confirms earlier work showing that DES implantation introduces small perturbations to the flow field surrounding the strut, causing drug-rich recirculating flow proximal and distal to the stent strut. These regions effectively extend the contact area of drug with the mural surface and therefore act to enhance drug uptake into the tissue below [2]. Studies of transient drug release in steady flow demonstrated that this flow-mediated drug deposition was time-dependent and ultimately a result of the local kinetics of the drug carrier [1].

In another study, pulsatile flow was shown to introduce recirculation regions surrounding the stent strut that were temporally periodic in length [13]. The latter study considered drug concentration as a constant source (i.e.  $c(t) = C_0$ ) on the surface of the strut therefore neglecting transient phenomena of drug release from the stent strut. The results in this study confirm the relationship between transient drug release *and* pulsatile flow, presenting a complete picture of dynamic drug elution and arterial wall drug uptake and distribution. Here the drug concentration profile in the recirculating region was consistent with pooling of a large proportion of the released drug with minimal dilution over time. In turn, this asymmetric pooling of drug was shown to result in a spatially variable distribution of drug in the tissue below. In this flow instance there was larger accumulation in the distal segment.

It is also important to note that owing to the large aspect ratio of the strut, the flow mediated effects were not significant to the overall tissue drug deposition when compared with those as a result of direct contact with the wall. The wider the stent strut, the greater the contact with the wall and therefore greater drug delivery to the vessel wall as a result of diffusion. At the same time there would also be less interruption with the near wall flow field and therefore a decrease in the flow mediated effects, as the strut has the effect of lying almost flat against the wall.

Further experimental work will consider the effects of these geometry influences as well using multiple strut configurations, more complex drug release strategies and possibly the interaction of flow mediated drug deposition with more intricate tissue mechanics.

## REFERENCES

- [1] B. Balakrishnan, J.F. Dooley, G. Kopia, and E.R. Edelman, "Intravascular drug release kinetics dictate arterial drug deposition, retention, and distribution," *Journal of Controlled Release*, vol. 123, pp. 100-108, 2007.
- [2] B. Balakrishnan, A.R. Tzafiriri, P. Seifert, A. Groothuis, C. Rogers, and E.R. Edelman, "Strut position, blood flow, and drug deposition - Implications for single and overlapping drug-eluting stents," *Circulation*, vol. 111, pp. 2958-2965, 2005.
- [3] M.A. Lovich, C. Creel, K. Hong, C.W. Hwang, and E.R. Edelman, "Carrier proteins determine local pharmacokinetics and arterial distribution of paclitaxel," *Journal of Pharmaceutical Sciences*, vol. 90, pp. 1324-1335, 2001.
- [4] C.J. Creel, M.A. Lovich, and E.R. Edelman, "Arterial paclitaxel distribution and deposition," *Circulation Research*, vol. 86, (no. 8), pp. 879-884, 2000.
- [5] C.W. Hwang, D. Wu, and E.R. Edelman, "Physiological transport forces govern drug distribution for stent-based delivery," *Circulation*, vol. 104, pp. 600-605, 2001.
- [6] M. Zamir, *The Physics of Pulsatile Flow*, New York: Springer-Verlag, 2000.
- [7] J.E. Moore Jr, D.N. Ku, C.K. Zarins, and S. Glagov, "Pulsatile flow visualization in the abdominal aorta under differing physiologic conditions: Implications for increased susceptibility to atherosclerosis," *Journal of Biomechanical Engineering*, vol. 114, pp. 391-397, 1992.
- [8] N.S. Cheng, "Formula for the viscosity of a glycerol-water mixture," *Ind. Eng. Chem. Res.*, vol. 47, (no. 9), pp. 3285-3288, May 2008.
- [9] S.J. Bryant, K.A. Davis-Arehart, N. Luo, R.K. Shoemaker, J.A. Arthur, and K.S. Anseth, "Synthesis and characterization of photopolymerized multifunctional hydrogels: Water-soluble poly(vinyl alcohol) and chondroitin sulfate macromers for chondrocyte encapsulation," *Macromolecules*, vol. 37, (no. 18), pp. 6726-6733, Sep 7 2004.
- [10] M.A. Lovich and E.R. Edelman, "Mechanisms of Transmural Heparin Transport in the Rat Abdominal-Aorta after Local Vascular Delivery," *Circulation Research*, vol. 77, (no. 6), pp. 1143-1150, Dec 1995.
- [11] A.S. Hickey and N.A. Peppas, "Solute diffusion in poly(vinyl alcohol) poly(acrylic acid) composite membranes prepared by freezing/thawing techniques," *Polymer*, vol. 38, (no. 24), pp. 5931-5936, Nov 1997.
- [12] W.M. Saltzman, *Drug Delivery: Engineering Principles for Drug Delivery*, New York: Oxford University Press, 2001.
- [13] V.B. Kolachalama, A.R. Tzafiriri, D.Y. Arifin, and E.R. Edelman, "Luminal flow patterns dictate arterial drug deposition in stent-based delivery," *Journal of Controlled Release*, vol. 133, pp. 24-30, 2009.